

Accounting for slotted cylindrical anodes in current inferences on pulsed power drivers

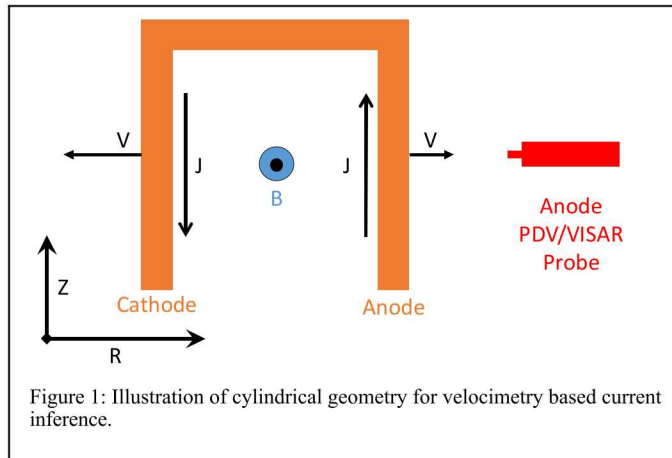
Andrew Porwitzky and Justin Brown
Sandia National Laboratories
Albuquerque, NM 87185
ajporwi@sandia.gov

Abstract—For over a decade, velocimetry based techniques have been used to infer the electrical current delivered to dynamic materials properties experiments on pulsed power drivers such as the Z Machine. Though originally developed for planar load geometries, in recent years inferring the current delivered to cylindrical coaxial loads has become a valuable diagnostic tool for numerous platforms. Previous work summarized uncertainties that can propagate through the current inference technique when applied to cylindrical anodes. The present work compensates for a known source of error generated when openings (slots) are cut into the cylindrical anode to allow optical diagnostic access to the load anode/cathode gap.

Keywords—Z Machine; pulsed power; load current diagnostic; velocimetry; MHD; power flow;

I. INTRODUCTION

For over a decade, velocimetry based techniques have been used to infer the electrical current delivered to dynamic materials properties experiments on pulsed power drivers such as the Z Machine (Z) at Sandia National Laboratories [1]. Though originally developed for planar load geometries, in recent years inferring the current delivered to cylindrical coaxial loads has become a valuable diagnostic tool for numerous platforms including MagLIF [2], [3], [4]. The process for determining a load current from velocimetry data is colloquially referred to as “unfolding a current” or simply that one has done an “unfold.” The standard method for determining current on a pulsed power machine is to use B-dots, but a scale factor is necessary to convert a measured magnetic field to an associated current. Calibration methods have been developed, though the presence of the scale factor can lead to some ambiguity [5]. In unfolds of planar geometries this scale factor also exists, as it is magnetic field that is inferred directly. In cylindrical coaxial geometry the boundary conditions are such that current can be inferred directly, with the scale factor simplified by the coaxial geometry. Additionally, B-dots can pick up extraneous magnetic fields, whereas velocimetry techniques are based on the application of highly localized forces. As such, in the last few years velocimetry based current inferences have become the most trusted current diagnostic on Z, while a quantitative error analysis has yet to be performed. This work adds to an ongoing uncertainty quantification effort.



Whether in planar or cylindrical geometry, the basic unfold technique is the same. The geometry relevant for a cylindrical unfold is illustrated in Figure 1, with the current flowing through the conductor on one side and free surface velocity measured on the opposite side. Velocity information can be acquired via photon Doppler velocimetry (PDV) [6] and/or velocity interferometry system for any reflector (VISAR) [7]. Surface velocity is then fed into a multiphysics modeling code (Alegria [8] is used here) where the conducting surface is represented in cylindrical geometry as a one-dimensional (1D) Lagrangian block with a time varying current imposed as a boundary condition on one side, and a Lagrangian tracer reproducing the velocimetry output on the opposite side. A non-linear least squares optimization is run on the time varying current using the Dakota optimization software [9] to find the current that will reproduce the experimentally measured velocity. Note that the resulting unfolded current is highly dependent on the material models used to represent the conductor, thus it is important to use materials for which well validated models exist. The DMP program at Sandia National Laboratories has developed validated models for aluminum which are used in both planar and cylindrical experiments on Z.

In the present work we will briefly summarize recently published uncertainty quantification efforts before adding an important new correction to the unfold method for slotted anode geometries.

II. SUMMARY OF PUBLISHED WORK

Recently published work addressed a variety of sources of error in a cylindrical unfold including uncertainty in the underlying velocity measurements and sensitivity of the unfold method at low pressures [10]. Since the current unfold is anchored to reality by the experimentally measured anode velocity, any uncertainty in velocity can have a significant effect on the unfold. VISAR/PDV uncertainty (noise) is generally less than 20 m/s, which is a small fraction of the overall uncertainty. The nonlinear least squares method itself has uncertainty, but it was found that together with the velocity noise these two terms represent less than 100 kA of uncertainty on the final unfold.

The largest source of velocimetry uncertainty was found to be target concentricity. For a cylindrical anode of inner radius R_a carrying electric current I centered on the origin, a non-concentric cathode whose center is offset distance x toward the measurement probe will experience a stronger magnetic field according to

$$B(x) = \frac{\mu_o I}{2\pi (R_a - x)} \quad (1)$$

which results in a higher velocity than would occur with perfect target concentricity. For a reasonable concentricity offset as determined from the specified machining tolerances of the Z target, it was found that current uncertainties of a few percent can result [10].

When all the various current uncertainties are taken into account, a relation was developed that can easily be incorporated into an unfold procedure. For uncertainty estimates calculated for the reference experiment used in [10] we found that at high current loads ($I > 10$ MA) unfold uncertainty is less than 3%. A detailed accounting of uncertainty vs current is shown in Table I.

TABLE I: Selected uncertainties from [10] as well as the load current experienced on Z3099. Note that at high current the uncertainty is dominated by the concentricity offset represented by Equation 1.

I (MA)	dI (kA)	dI/I	I (MA)	dI (kA)	dI/I
0	203	∞	10	239	2.39%
2	208	10.42%	12	286	2.38%
4	203	5.07%	14	333	2.38%
6	152	2.53%	16	380	2.37%
8	192	2.40%	18	427	2.37%

This uncertainty quantification assumes that there are no systematic errors in the method. However, for some experiments the method possesses a known error that can be corrected, namely the affect of a non-enclosed cylindrical anode.

III. SLOTTED ANODE RETURN CANS

From a computational modeling standpoint, the force moving the anode and cathode surfaces is generated not by the electric current, but by the magnetic pressure induced by that current. In a planar geometry, the unfold method identified the magnetic field (B), rather than the current (I). For a cylindrical

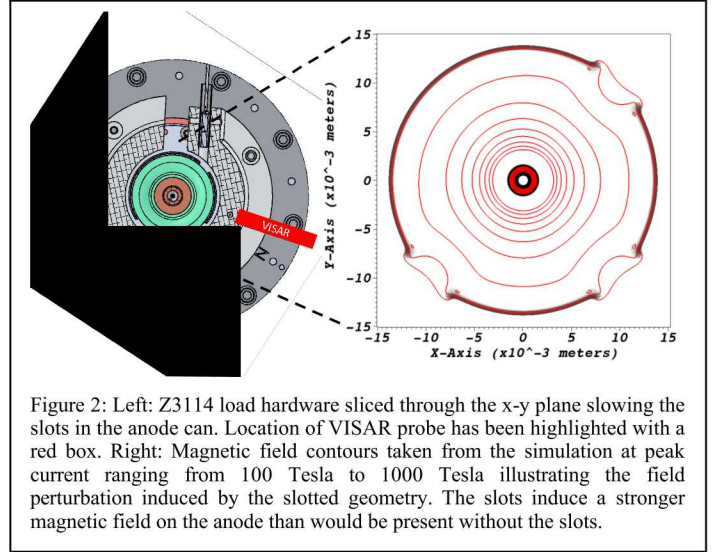


Figure 2: Left: Z3114 load hardware sliced through the x-y plane showing the slots in the anode can. Location of VISAR probe has been highlighted with a red box. Right: Magnetic field contours taken from the simulation at peak current ranging from 100 Tesla to 1000 Tesla illustrating the field perturbation induced by the slotted geometry. The slots induce a stronger magnetic field on the anode than would be present without the slots.

geometry, a convenient scaling relation exists for the magnetic field on the anode surface given by Equation 1 with $x=0$. In the multiphysics code Alegra, as the anode is moved outwards under magnetic pressure the anode inner radius (R_a) is updated at every computational time step, thus allowing the scale factor relating I to B to change appropriately.

Equation 1 defines the magnetic field generated outside of a current carrying wire and fails if local perturbations of the magnetic field exist for geometric reasons. Let us adopt the geometry of another Z experiment with a similar current pulse to Z3099 but with a slotted anode geometry. Z3114 possessed three angular slots of 17.1° full angle centered at 0° , 90° , and 180° in order to provide optical diagnostic access to the anode/cathode gap. Alegra can be used to simulate the two-dimensional (2D) geometry evolution as a slice through the $R-\theta$ plane. Magnetic field contours at peak current (approximately 14 MA) are shown in Figure 2 along with a rendering of the hardware geometry. It is easy to see that if $x=0$ then Equation 1 generates circular magnetic field equipotentials centered on the origin. The slots in the current carrying anode generate magnetic field perturbations which enhance the magnetic field at the cathode surface between the slots. For this experiment the slots were designed such that the magnetic field relaxes to uniformity to within a fraction of a percent at the cathode surface, thus no implosion asymmetry is generated. It is impossible, however, to prevent field asymmetry on the anode surface, even far from the slots. Let us consider what affect this field asymmetry has on the anode current unfold method.

Since the slots induce a magnetic field asymmetry on the anode inner surface, the magnetic pressure experienced at each angular location of the anode is now slightly different. Plotting the magnetic field equipotentials for a closed anode and overlaying those with the equipotentials in Figure 2 indicates that the slotted geometry induces a higher magnetic field on the inside of the anode. This is because the slots locally decrease the magnetic field around themselves, which causes the magnetic field to be pinched to higher values along the solid anode inner surface. The result of this perturbation is insidious. With the local magnetic field higher the force on the anode

surface is bigger, meaning that the resulting anode velocity will be larger. Without a scale factor correction, the 1D unfold method will use Equation 1 to calculate the I from the necessary B and lead to a larger current than actually flowed through the anode. Unless compensated for, simply cutting slots in the anode geometry will make it appear that more current reached the Z target. In fact, it was observed on a recent Z experiment with a particularly aggressive slot geometry that the unfolded load current (before slotted anode correction) was several mega-amps higher than the current measured at the Z MITL, before typical loss mechanisms kick in. Thus awareness and use of the slotted anode correction is necessary not just for accuracy but to ensure confidence in the unfold method as a whole.

IV. A METHOD FOR CORRECTION

As stated, the 1D unfold method assumes a cylindrical scale factor given by Equation 1 for connecting B to I which results in an overestimation of I for slotted anodes. Recall that the unfold method is anchored to reality by the experimentally measured anode expansion velocity, thus the local B inferred by the unfold is correct as that magnetic pressure successfully reproduces the experimental velocity. (We are assuming a numerically converged unfold with acceptable residuals [10].) The fact that it is the local B that is correct is key; it is necessary to know the location of the velocity measurement in relation to the slotted geometry in order to extract the magnetic field from a 2D $R-\theta$ simulation. For instance, the magnetic field in Figure 2 on the inner surface of the anode at approximate $x-y$ location (13 mm, 0 mm) is higher than the field at (-8 mm, 10 mm), because the closer two slots are the higher the local field pinching between them. The location of the velocimetry probe is highlighted in Figure 2 as the red box labeled “VISAR” and corresponds to a region of rather strong field enhancement.

The method for connecting 1D current unfolds for slotted anode geometries is as follows and will be described in detail subsequently.

1. Perform a “normal” 1D unfold method, which assumes a closed anode scale factor (Equation 1) but is close to the correct scale factor because of the gross assumption of cylindrical geometry. This results in current I_{1D} , which will be an overestimation of the true current for slotted geometries. Extract the B generated on the anode surface in the simulation, giving B_{1D} .
2. Run a 2D $R-\theta$ simulation (as shown in Figure 2) with I_{1D} , tracking B along the inner surface of the anode corresponding to the location where the velocity data was recorded in the experiment; we will call this B_{2D} .
3. Calculate a corrected scale factor for I_{1D} using B_{1D} and B_{2D} . Note that since B_{1D} accurately produces the experimental anode velocity it is B_{1D} which anchors us to reality and is the desired magnetic field on the inner surface of the slotted anode. We will call the corrected (true) current I^* . Since the 1D scale factor is very close to the perturbed true scale factor, this

procedure, though iterative, need only be done once to converge to the proper $B(I)$ functional relationship. Confirmation can be obtained by running a 2D $R-\theta$ simulation with I^* to find that $B_{2D}^* = B_{1D}$.

This method was designed to be as efficient as possible given the large number of current unfolds that are now being performed on slotted anode geometries as part of the Z inertial confinement fusion program. Note that because I^* is the current that results from the unfold procedure, all uncertainties previously outlined in [10] can be applied to it directly.

V. APPLYING THE CORRECTION TO Z3114

We will now use Z experiment Z3114, whose geometry is illustrated in Figure 2, as an example case for the slotted anode correction using the method outlined in Section IV. The experimentally measured velocity at the location specified in Figure 2 is shown along with the 1D (uncorrected) current unfold in Figure 3. The timing difference between the current and the velocity is due to the acoustic wave propagation speed through the initially 450 μm thick aluminum anode. Fluctuations visible in the 1D current unfold are due to uncertainties characterized in [10].

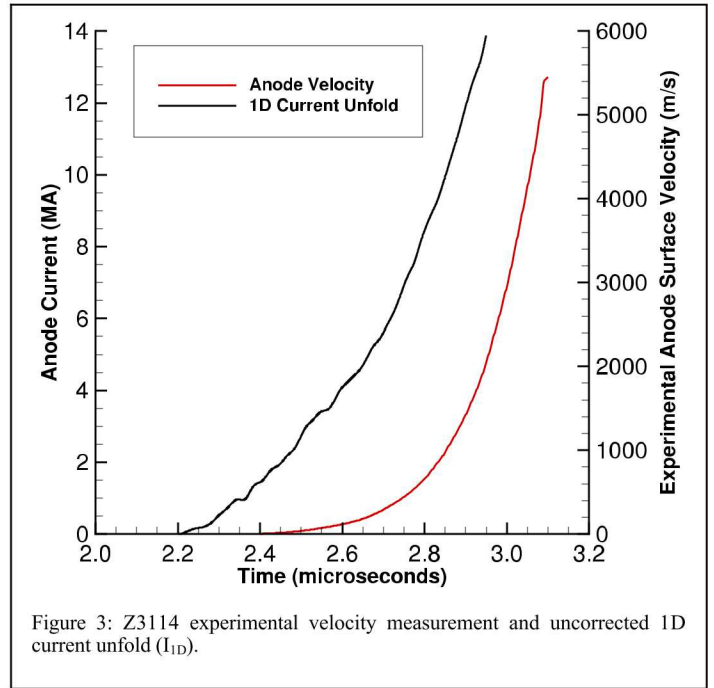


Figure 3: Z3114 experimental velocity measurement and uncorrected 1D current unfold (I_{1D}).

We now run I_{1D} through our 2D slotted geometry simulation illustrated in Figure 2. Lineouts following the VISAR probe line of sight are taken for magnetic field and anode material volume fraction. These lineouts are combined in order to track the magnetic field on the inner liner surface on the sight line of the VISAR probe. From this we can generate the local driving magnetic field as a function of time for the liner in the slotted geometry (B_{2D}). B_{2D} is larger than B_{1D} since the scale factor assumed in the 1D unfold is incorrect. From Equation 1 we can see that scale factor is defined simply as $S=B/I$, so given the total I and the B at a given location we can calculate the local scale factor. To find the corrected current I^* we calculate the slotted (correct) local scale factor to be $S^*=$

B_{2D}/I_{1D} . With the local scale factor known, the corrected current is $I^*=B_{1D}/S^*$. This procedure is iterative, though because B_{1D} anchors us to the experimental result and B_{1D} and I_{1D} were related by the cylindrical scale factor (of which the slotted geometry is a perturbation) the method converges in one iteration. As a check, running I^* through the 2D slotted geometry and performing the lineout procedure reproduces B_{1D} .

The final result of the current correction is shown in Figure 4 along with the original 1D unfold for comparison. Here we include error bars applied to I^* using the method outlined in [10]. Early in the current pulse (before much motion occurs) the inaccuracy of the scale factor is a minor affect. As the current grows and the liner moves, the enhanced force associated with the magnetic field pinching as a result of the slots more significantly accelerates the liner, compounding the error. At peak current the difference is 6.3%, or a nearly 800 kA overestimation of the load current.

Some insight into the importance of performing a full 2D simulation can be gained by plotting the time dependent scale factors. Figure 5 shows the time evolution of various scale factors, including the analytical form calculated from Equation 1 using the R_a location extracted as part of the procedure to calculate the 1D scale factor (S_{1D}). Significant noise occurs before 2.6 μ s which corresponds to 4 MA on our current pulse, a region below which enhanced uncertainties exist in the current unfold [10]. Looking later in time, the 1D scale factor from the simulation is smaller than the analytical form because the presence of the current carrying anode decreases the magnetic field near the anode surface, which is where we are looking. Both the analytical and the 1D scale factors preserve the decreasing character expected since $S \sim 1/R_a$, and R_a increases in time as the anode expands under magnetic pressure. The red trace in Figure 5 is the scale factor S^* , or the scale factor at the VISAR relevant location of the slotted

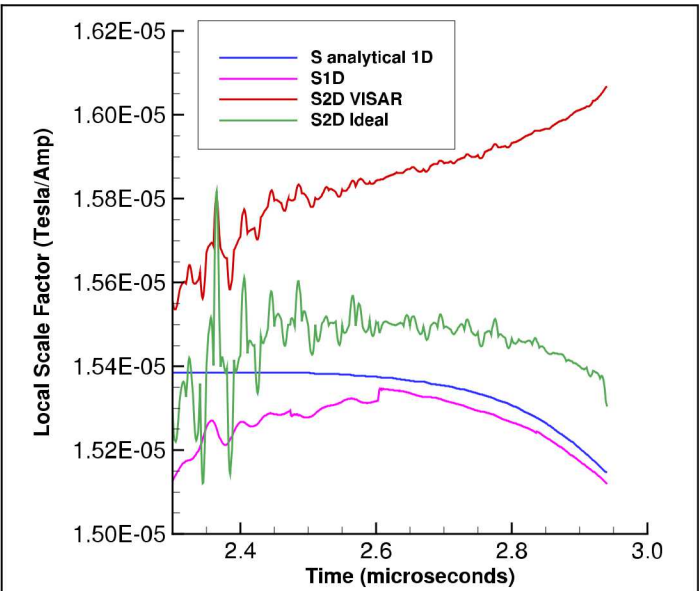


Figure 5: Local scale factors for the enclosed and slotted anode geometries. Note that in the case of the VISAR relevant location, the fundamental trend of the scale factor changes due to proximity of the slot.

anode, which actually increases as a function of time. It would appear that we are capturing an edge effect due to the deformation of the nearby slot late in time (visible as a curling outwards of the liner material on the bottom right of Figure 2). If that is the cause, then we would expect a scale factor extracted far from any slots to recover the decreasing trend of the analytical scale factor. Lineouts were taken -45° from vertical in Figure 2 and plotted in Figure 5 as “S2D Ideal” since this location would be the ideal place to make a VISAR measurement to ensure minimum deviation from the analytical scale factor. Most of the $1/R_a$ dependence is recovered, though the correction method should still be applied. We can thus see that the slotted geometry can fundamentally alter the evolution behavior of the scale factor beyond what might be expected.

VI. CONCLUSION

In recent years, velocimetry based load current inference has become the most accurate current diagnostic method for multi-mega-amp pulsed power drivers. One of its advantages is characterizable uncertainties from various sources. Complexities in the analysis arise when cutting openings in the cylindrical anode, altering the scale factor from what is assumed in the one-dimensional current unfold. However, this change can be compensated for with existing magnetohydrodynamic multiphysics codes. A correction method has been developed which, once performed, allows previously characterized uncertainties to be applied. This work represents another step in an ongoing effort to fully characterize all sources of uncertainty for velocimetry-based current inferences in cylindrical geometries.

ACKNOWLEDGMENT

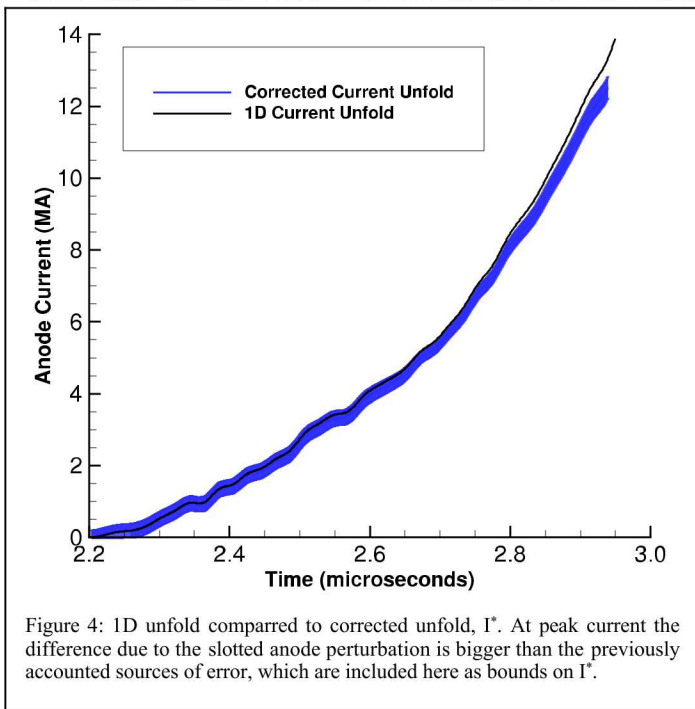


Figure 4: 1D unfold compared to corrected unfold, I^* . At peak current the difference due to the slotted anode perturbation is bigger than the previously accounted sources of error, which are included here as bounds on I^* .

Thanks go to Matt Gomez for the initial request to investigate slotted anode can unfold accuracy, and to Lynn Twyeffort for CAD design of all the authors' cylindrical experimental loads for Z. We sincerely thank the staff, technologists, and management that make experiments on Z possible. Sandia National Laboratories is a multimission laboratory managed and operated by National Technology and Engineering Solutions of Sandia LLC, a wholly owned subsidiary of Honeywell International Inc. for the U.S. Department of Energy's National Nuclear Security Administration under contract DE-NA0003525.

REFERENCES

- [1] R.W. Lemke et al., "Magnetically accelerated, ultrahigh velocity flyer plates for shock wave experiments," *Journal of Applied Physics* 98, 073530 (2005).
- [2] R.W. Lemke et al., "Probing off-Hugoniot states in Ta, Cu, and Al to 1000 GPa compression with magnetically driven liner implosions," *Journal of Applied Physics* 119, (2016).
- [3] S.A. Slutz and R.A. Vesey, "High-gain magnetized inertial fusion," *Physics Review Letters* 108, 025003 (2012).
- [4] M.R. Gomez et al., "Experimental demonstration of fusion-relevant conditions in magnetized liner inertial fusion," *Physics Review Letters* 113, 155003 (2014).
- [5] T.C. Wagoner et al., "Differential-output b-dot and d-dot monitors for current and voltage measurements on a 20-ma, 3-mv pulsed-power accelerator," *Phys. Rev. ST Accel. Beams* 11, 100401 (2008).
- [6] O.T. Strand, D.R. Goosman, C.Martinez, T.L. Whitworth, and W.W. Kuhlow, "Compact system for high-speed velocimetry using heterodyne techniques," *Review of Scientific Instruments* 77, 083108 (2006).
- [7] L.M. Barker and R.E. Hollenbach, "Laser interferometer for measuring high velocities of any reflecting surface," *Journal of Applied Physics* 43, 4669-4675 (1972).
- [8] A. Robinson et al., "Alegra: An arbitrary lagrangian-eulerian multimaterial, multiphysics code," 46th AIAA Aerospace Sciences Meeting and Exhibit, Aerospace Sciences Meetings (2008).
- [9] B. Adams, et al., "Dakota, a multilevel parallel object-oriented framework for design optimization, parameter estimation, uncertainty quantification, and sensitivity analysis: version 6.0 user's manual," Sandia Technical Report, SAND2014-4633 (2014).
- [10] A. Porwitzky and J. Brown, "Uncertainties in cylindrical anode current inferences on pulsed power drivers," accepted for publication in *Physics of Plasmas* (2018).